




## ARTICLE

# Eliciting the antitumor immune response with a conditionally activated PD-L1 targeting antibody analyzed with a quantitative systems pharmacology model

Alberto Ippolito<sup>1</sup> | Hanwen Wang<sup>1</sup>  | Yu Zhang<sup>1</sup>  | Vahideh Vakil<sup>2</sup> |  
Hojjat Bazzazi<sup>2</sup> | Aleksander S. Popel<sup>1,3</sup> 

<sup>1</sup>Department of Biomedical Engineering, Johns Hopkins University School of Medicine, Baltimore, Maryland, USA

<sup>2</sup>Clinical and Quantitative Pharmacology, CytomX Therapeutics, Inc., South San Francisco, California, USA

<sup>3</sup>Department of Oncology, and the Sidney Kimmel Comprehensive Cancer Center, Johns Hopkins University School of Medicine, Baltimore, Maryland, USA

## Correspondence

Alberto Ippolito, Department of Biomedical Engineering, Johns Hopkins University School of Medicine, Baltimore, MD 21205, USA.  
Email: [alberto.vippolito@gmail.com](mailto:alberto.vippolito@gmail.com)

## Present address

Hojjat Bazzazi, Moderna Therapeutics, Cambridge, MA, USA

## Abstract

Conditionally activated molecules, such as Probody therapeutics (PbTx), have recently been investigated to improve antitumoral response while reducing systemic toxicity. PbTx are engineered to be proteolytically activated by proteases that are preferentially active locally in the tumor microenvironment (TME). Here, we perform an exploratory study using our recently published quantitative systems pharmacology model, previously validated for other drugs, to evaluate the effectiveness and targeting specificity of an anti-PD-L1 PbTx compared to the non-modified antibody. We have informed the model using the PbTx dynamics and pharmacokinetics published in the literature for anti-PD-L1 in patients with triple-negative breast cancer (TNBC). Our results suggest masking of the antibody slightly decreases its efficacy, while increasing the localization of active therapeutic component in the TME. We also perform a parameter optimization for the PbTx design and drug dosing regimens to maximize the response rate. Although our results are specific to the case of TNBC, our findings are generalizable to any conditionally activated PbTx molecule in solid tumors and suggest that design of a highly effective and selective PbTx is feasible.

## Study Highlights

## WHAT IS THE CURRENT KNOWLEDGE ON THE TOPIC?

Conditionally activated antibodies, such as Probody therapeutic (PbTx) antibodies, are molecules designed to be selectively activated in the tumor microenvironment. Recently, a phase I clinical trial has demonstrated the activity of pacmilimab, a PbTx with anti-PD-L1 immune-checkpoint properties, in solid tumors.

Hojjat Bazzazi and Aleksander S. Popel jointly supervised this work.

This is an open access article under the terms of the [Creative Commons Attribution-NonCommercial](https://creativecommons.org/licenses/by-nc/4.0/) License, which permits use, distribution and reproduction in any medium, provided the original work is properly cited and is not used for commercial purposes.

© 2023 The Authors. *CPT: Pharmacometrics & Systems Pharmacology* published by Wiley Periodicals LLC on behalf of American Society for Clinical Pharmacology and Therapeutics.

### WHAT QUESTION DOES THIS STUDY ADDRESS?

Here, we use a quantitative systems pharmacology model of immuno-oncology (QSP-IO), previously validated for anti-PD-L1 therapies in patients with triple-negative breast cancer, and inform the model using previously published literature describing the PbTx dynamics and perform an exploratory investigation of this molecule.

### WHAT DOES THIS STUDY ADD TO OUR KNOWLEDGE?

This work represents the first application of a QSP-IO platform to describe the activation of antitumor immune response by a PD-L1 targeting PbTx. The application of the platform in exploring antitumor response with the PbTx provides key clinical predictions on the PbTx's activity, and important biomarkers characterizing the patient's response, as well as an investigation into how this response depends on the PbTx kinetic parameters and the dosing schedule.

### HOW MIGHT THIS CHANGE DRUG DISCOVERY, DEVELOPMENT, AND/OR THERAPEUTICS?

The results obtained from our simulations suggest both possible advancements in the drug design as well as alternative dosing amounts and frequencies to maximize the drug's effectiveness while maintaining a low toxicity level.

## INTRODUCTION

Conditional activation of drugs in the tumor microenvironment (TME) has emerged as a potential strategy for cancer immunotherapy in recent years. These approaches consist of exploiting selected properties of the TME to design molecules that are specifically activated by and target cancer cells. There are different approaches for targeted activation of the molecules in the tumor. One approach, utilized in Probody therapeutics (PbTx), exploits high protease activity in the tumor compared to normal tissue<sup>1</sup> and involves designing molecules that are activated by tumor-resident proteases.

One PbTx design consists of attaching a peptide mask via a substrate linker to the active site of the molecule.<sup>2</sup> The peptide mask is capable of stochastically and reversibly covering the molecule's active site. The substrate is designed to be cleavable by proteases expected to be highly active in the tumor, such as tumor-associated serine protease matriptase, urokinase plasminogen activator, and cysteine protease legumain.<sup>3</sup> These enzymes digest the substrate linker, freeing the mask, and, thus, revealing the active site of the molecule. Because of the active protease-rich environment of the tumor, the PbTx is more likely to become activated in the TME compared to healthy tissues. PbTx uses a versatile design that is applicable to a variety of biologically active molecules, including antibodies, antibody-drug conjugates, and bispecific modality molecules.<sup>2</sup> Among these, CX-072 PbTx, also known as pacmilimab, is a conditionally activated immune checkpoint inhibitor of PD-L1.<sup>4</sup> Pacmilimab was tested

in a phase I study to provide a preliminary evaluation of dose and schedule<sup>4-6</sup> in patients with solid tumors. This pan-cancer trial suggested that a biweekly administration dose of 10 mg/kg provided the maximal response while inducing moderate to light toxicity.

In parallel to the clinical trial, quantitative systems pharmacology (QSP) models have been developed to describe and predict the kinetics of pacmilimab.<sup>7,8</sup> Specifically, the model by Stroh et al.<sup>7</sup> is a three-compartment QSP model with plasma, peripheral tissue, and tumor compartments that include the transition between different states of the PbTx as well as the binding to receptors. This model was then adapted specifically to pacmilimab<sup>8</sup> where the preliminary data from clinical trials was used to calibrate the model pharmacokinetic (PK) and pharmacodynamic (PD) relations. However, whereas this model fully describes the PKs/PDs of the molecule, it does not include the downstream effects of the PD-L1 checkpoint inhibition, such as the resulting T cell activation and tumor killing.

In the present study, we construct a mechanistic computational model to investigate activation of antitumor immune response to pacmilimab. In the current state-of-the-art, QSP models are routinely used to predict and explain the effects of therapies on populations of virtual patients.<sup>9</sup> QSP models inform a mechanistic framework with the PKs/PDs of the therapy to describe, for example, the distribution or activity of a compound.<sup>10</sup> Although QSP models describing the PbTx PKs/PDs have been published,<sup>7,8</sup> there have not been any models describing the immuno-oncologic (IO) response to these drugs.

Here, we deploy a recently published QSP-IO platform model validated for other drugs for an exploratory study of pacmilimab.<sup>11</sup> We model the role of this drug in activation of the immune response in patients with triple-negative breast cancer (TNBC). We chose TNBC because the model was previously validated for this cancer type and this was one of the cancer types present in the published phase I trial.<sup>6</sup> We have incorporated PbTx state transition dynamics<sup>7</sup> and PKs in the QSP-IO platform and tested the response in patients with TNBC based on a published model<sup>11</sup> for anti-PD-L1 therapy in this cancer type. Additionally, we have extended the QSP-IO model by introducing out-of-synapse dynamics (interactions between the drug and ligands happening outside of the cellular synapse). the previous model only considered drug-receptor interactions within the immunological synapse.<sup>11-13</sup> We validate and use this QSP-IO platform for the application of conditionally masked checkpoint inhibitors. Our results suggest masking the PD-L1 targeting antibody has modest impact on efficacy, while improving the localization of active therapeutic in the TME. We also perform a global parameter sensitivity analysis to suggest mechanisms or modifications to the molecule that may maximize the response rate of virtual patients to the PbTx. Although the current results are relevant to TNBC, we can envision parametrizing the model using other cancer types to perform similar simulations for the response to PbTx. The current work provides a framework for incorporating PbTx into the QSP-IO platform to investigate activation of antitumor immune response in a virtual patient setting.

## METHODS

### Overview of the QSP-IO model and addition of the out-of-synapse module

QSP-IO models are mechanistic frameworks used to predict population and individual responses to immune, chemo-, and combination therapies. Usually, the systems in question are divided into multiple compartments, each representing a different tissue or organ or their assemblies, inside which a set of explicitly modeled molecular or cellular species can interact or move between compartments. In particular, QSP-IO models are informed with the PK/PD relations governing the drug as well as the interactions between the immune system and tumor cells. Each simulation is run for a different virtual patient (VP), which is the set of parameters describing the mechanistic relations or properties of each species and compartment. For each VP, some parameters are randomly selected from known physiologically relevant distributions to simulate inter-patient variability. Whereas each VP does not necessarily

represent a real patient, the resulting simulated cohort of multiple VPs yields a population average and single VP response to the selected therapy.

In this work, we implement the previously published QSP-IO model for the evaluation of pacmilimab monotherapy as the anti-PD-L1 immune checkpoint inhibitor.<sup>11</sup> Although we provide a detailed explanation of the theory and implementation in Appendix S1, here, we give a brief overview of the model.

The model used in our work, shown in Figure 1, contains four distinct compartments: the tumor, tumor-draining lymph node, peripheral, and central compartment. The tumor compartment contains cancer and stromal cells and is the location where the tumor interacts with the components of the immune system in the TME. The tumor-draining lymph nodes are the location where antigen presentation and T cell maturation occur. The peripheral compartment describes the rest of the body and it is generally used to describe unwanted activity of the therapy. Finally, the central compartment represents blood flow which connects all the compartments. Details on the PKs and PDs in each compartment are described in Appendix S1.

The model contains the dynamics of several different cell types from the immune system as well as those of the tumor. These dynamics are divided into 11 different modules, each describing interactions for different cell's or a key molecular species' interactions. Within these modules, we explicitly model the maturation, activation, depletion, and death of CD-8, CD-4, and regulatory (Treg) T cells. These cells come into contact with mature antigen-presenting cells (APCs) arriving from the TME. These APCs mature in response to the release of cytokines in the TME. Additionally, macrophages in the M1 and M2 configurations are also modeled in the TME. The interactions between these different cells are ascribed to the synaptic compartments. This compartment includes all the different ligands used for immune-regulatory actions, such as PD-L1, PD-1, PD-L2, CTLA4, CD28, TCR, MHC, and CD80.

Of the 11 modules, 10 were previously implemented by Wang et al.<sup>11</sup>; here, we also introduce an additional compartment to explicitly model the out-of-synapse dynamics. We explicitly include only PD-L1, because it is the only ligand that will interact with the PbTx, however, we want to emphasize that the same procedure can be applied to the other ligands, that is, CTLA4 and PD-1. We do not include binding between the downstream pathways of PD-L1 in the cell, but we recognize that these can lead to some additional dynamic effects as reported in literature.<sup>12</sup> We follow a similar approach for out-of-synapse compartment modeling as proposed by Bazzazi et al.<sup>13</sup> Whereas quantifying the differences between the ligand densities

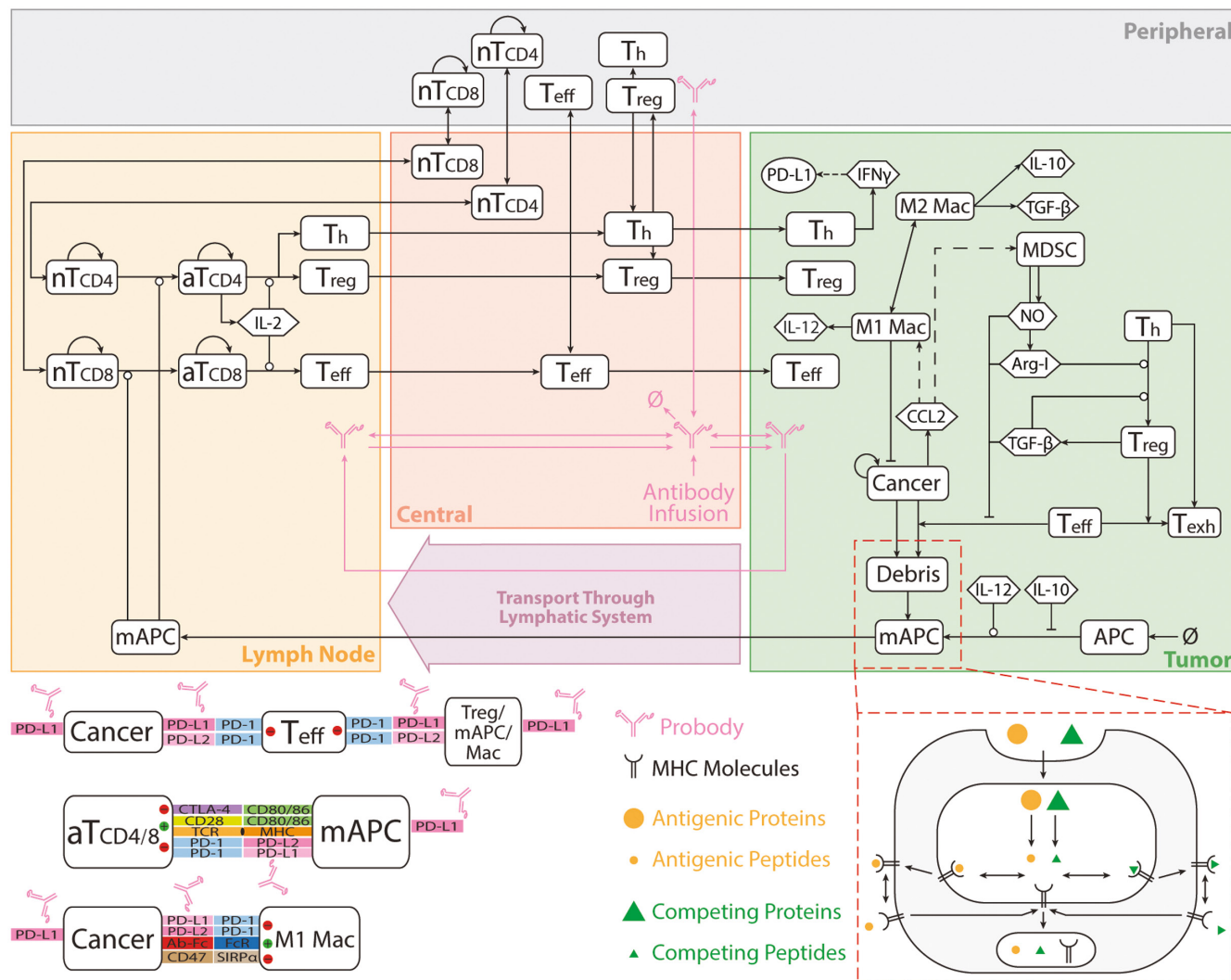


**FIGURE 1** Diagram detailing the quantitative systems pharmacology model used in this work. Compared to previously published study,<sup>11</sup> this model includes the out-of-synapse dynamics of PD-L1, as shown in the bottom left panel, as well as the Probody therapeutics (PbTx) dynamics.

inside and outside of the synapse, as well as the area that is definable as “synapse,” is still debated, here, we follow a procedure similar to Wang et al.<sup>11</sup> to model these two compartments. We assume that there is a baseline PD-L1/2 expression on cancer and immune cells, which can be up-regulated by IFN- $\gamma$  upon immune activation, based on the difference in measured PD-L1/2 expression in resting and activated immune cells.<sup>14</sup> Additionally, all ligands are allowed to interact with the PbTx, whereas only the ligands in the synaptic compartments are allowed to interact with ligands of other cells. We assume that there is no net diffusion between synapse and out-of-synapse, which means that we can consider the concentrations within each compartment as independent. We assume that all the other properties, such as interaction distances of ligands and the diffusive properties of the antibody, are the same as in the synapse. All the equations describing the synaptic

and out-of-synaptic binding are found in Appendix S1 (Equations S66-S68).

## Overview of the Probody therapeutic dynamics

The following is an overview of the PbTx dynamics and is explained in more in detail in Appendix S1. Although PbTx PK/PD have been previously published,<sup>7,8</sup> this work represents the first application of a QSP-IO platform to describe the activation of antitumor immune response by a PD-L1 targeting PbTx. Whereas the model complexity is further dealt with in the Supplementary Materials, here, our overview covers the key parameters that govern the PbTx mechanics (Equations S51–S65), that is, the cleavage and unmasking rates.



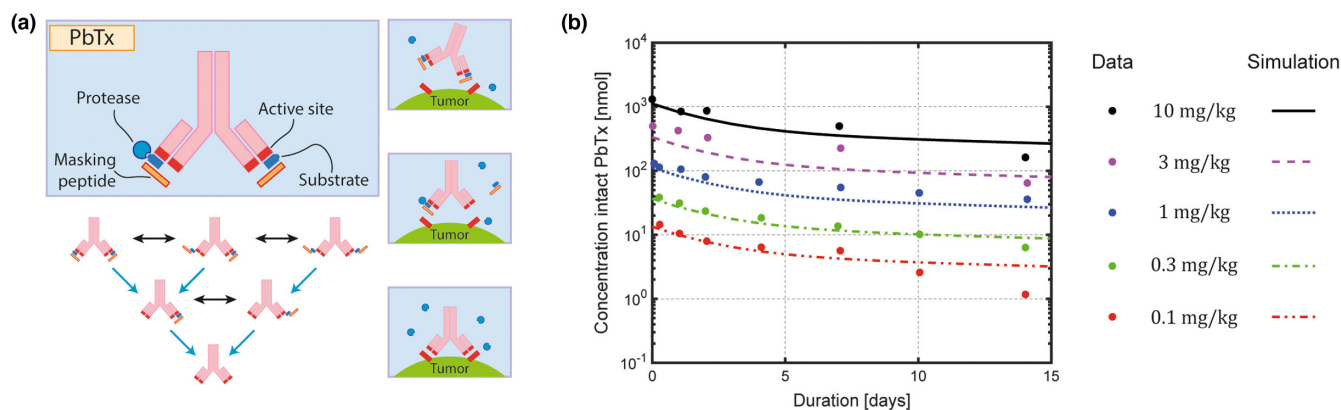


**FIGURE 2** (a) Cartoon demonstrating the PbTx dynamics described in ref. 7. The PbTx can exist in one of six possible states by either reversible unmasking or via irreversible mask cleavage by TME proteases. Five PbTx states are capable of binding with at least one target. Additionally, the side panels qualitatively describe how the mask cleavage occurs. (b) Model calibration to single dose PbTx data extracted averaged over the same 10,000 virtual patients for each dose.<sup>8</sup> PbTx, Probody therapeutics; TME, tumor microenvironment.

Pacmilimab is a PbTx that is an activatable anti-PDL1 antibody. It has a mask covering the active sites of the antibody component that is kept in proximity thereto by a cleavable substrate linker, as shown in Figure 2a. The PK model describing the PbTx dynamics has been described previously by Stroh et al.<sup>7</sup> Briefly, the mask is allowed to stochastically and reversibly shift and reveal the active site. This unmasking rate is governed by an equilibrium constant  $K_M$ , which is the likelihood that the mask will reveal the active site. If this were the only addition to the antibody, then the PbTx would just be a less active form of its parent solely due to the reduced exposure of the active site. However, this reduced exposure is made selective because the key property of the PbTx is that the substrate holding the mask is cleavable by proteases overexpressed in the TME. These proteases are tumor-associated serine protease matriptase, urokinase plasminogen activator, and cysteine protease legumain<sup>1</sup> for pacmilimab; however, it is possible to select other substrates that are digestible by different enzymes.<sup>15</sup> As shown in Figure 2a, these enzymes bind to the substrate and cleave it, freeing the mask from the antibody and, thus, irreversibly revealing the active site. The idea is that outside of the TME, where active proteases are rare, the PbTx is a minimally active version of the unmasked antibody while in the TME, thanks to the cleaving ability of the enzymes, the antibody is fully activated and can act with its full pharmacologic potential. Although the proteases are overexpressed by cancer cells and stromal cells in the tumor compared to healthy tissues, each cancer type demonstrates different level of expression.<sup>16</sup> Additionally, even within the same cancer type, there is a distribution of these active proteases. Thus, diverging from the previous PbTx models, we model the cleavage rate  $k_{cvg}$  as a patient-dependent parameter,

where the mean of  $k_{cvg}$  is set to the one reported value in literature.

We calibrate the model using data provided in Stroh et al.,<sup>8</sup> as shown in Figure 2b. In these experiments, a single injection of pacmilimab at doses 0.1, 0.3, 1, 3, and 10 mg/kg was administered. Initial calibration of the PKs of pacmilimab in patients was performed by visually comparing the observed blood-uncleaved pacmilimab concentration, obtained by liquid chromatography in tandem with mass spectrometry,<sup>8</sup> with the simulated one. We repeat the same simulations with our model and plot the observed data points along with the equivalent median simulation curves obtained from 100 VPs. We note that Stroh<sup>8</sup> showed that PbTx works for a representative Ab (anti-CD166). It showed overall systemic exposure but can be tweaked (by mask strength) to change uptake in peripheral and tumor tissues. In this work, we have assumed that the PK properties of the PbTx are the same as the ones for the naked anti-PD-L1 monotherapy reported in ref. 11.

## RESULTS AND DISCUSSION

### Pacmilimab's effectiveness is modestly different than the unmasked antibody

Now that we have calibrated the QSP-IO model with the PbTx molecule dynamics, we proceeded to evaluate the therapy in terms of effectiveness. The only reference clinical study of pacmilimab in TNBC is the phase I trial recently published.<sup>6</sup> The proposed dosing regimen based on the trial is 10 mg/kg every 2 weeks (q2w), as it optimized the trade-off between drug efficacy and safety. Higher doses, that is, 30 mg/kg administered q2w,

induced adverse reactions,<sup>6</sup> whereas lower doses, such as 3 mg/kg administered q2w, may be less efficacious. The duration of the therapies for 16 patients with TNBC varied from a few months up to 96 weeks. Following the suggested schedule, we thus simulate the dose regimen of 10 mg/kg administered q2w for a duration of 400 days, which is similar to other PD-L1 immune-checkpoint inhibitor therapies.<sup>17</sup> We proceed by simulating three cases for the same 10,000 VPs: untreated progression, unmasked antibody monotherapy, and PbTx monotherapy. The “untreated” case refers to allowing the dynamics of clinical progression to evolve without the addition of any external therapy. We assume that the length of these hypothetical untreated cases is the same as the therapy, that is, 400 days. The “unmasked antibody” monotherapy refers to injecting a fully cleaved (i.e., without both masks) antibody. We want to emphasize that the “unmasked” therapy is equivalent to the results of atezolizumab monotherapy reported in ref. 11. Because the unmasked antibody monotherapy will serve as the reference case, we assume that it will also be applied with the same dosing schedule as pacmilimab, that is, 10 mg/kg administered q2w.

In Figure 3a, we show the simulated percent change tumor size, as a ratio between the individual tumor volume at the end of the treatment and pretreatment, for selected representative 1000 VPs, chosen randomly from the 10,000 VP cohort, for the unmasked monotherapy. The percent change in tumor size is a common method for comparing the patient response to treatment.<sup>18</sup> Equivalently, in Figure 3b, we show the change in tumor size for pacmilimab monotherapy for the same 1000 patients. For both Figures 3a and 3b, we trace dotted limits at 20% and –30% following the RECIST 1.1 criteria.<sup>19</sup> Specifically, we label the regions of progressive disease, stable disease and partial/complete response, which represents the responders. Visually, the data in these figures suggest that the number of responders is slightly higher for unmasked monotherapy (8% vs. 6% in the masked monotherapy). To better quantify this, we show the equivalent RECIST category bar plots as percentages of the patient cohort in Figure 3c. Each bar contains an error bar defining the 95% confidence interval (CI) and the *p* values between the entire dataset for different cases (untreated, unmasked, and PbTx therapy) are also shown, see Appendix S1. Results suggest that the number of responders is slightly higher

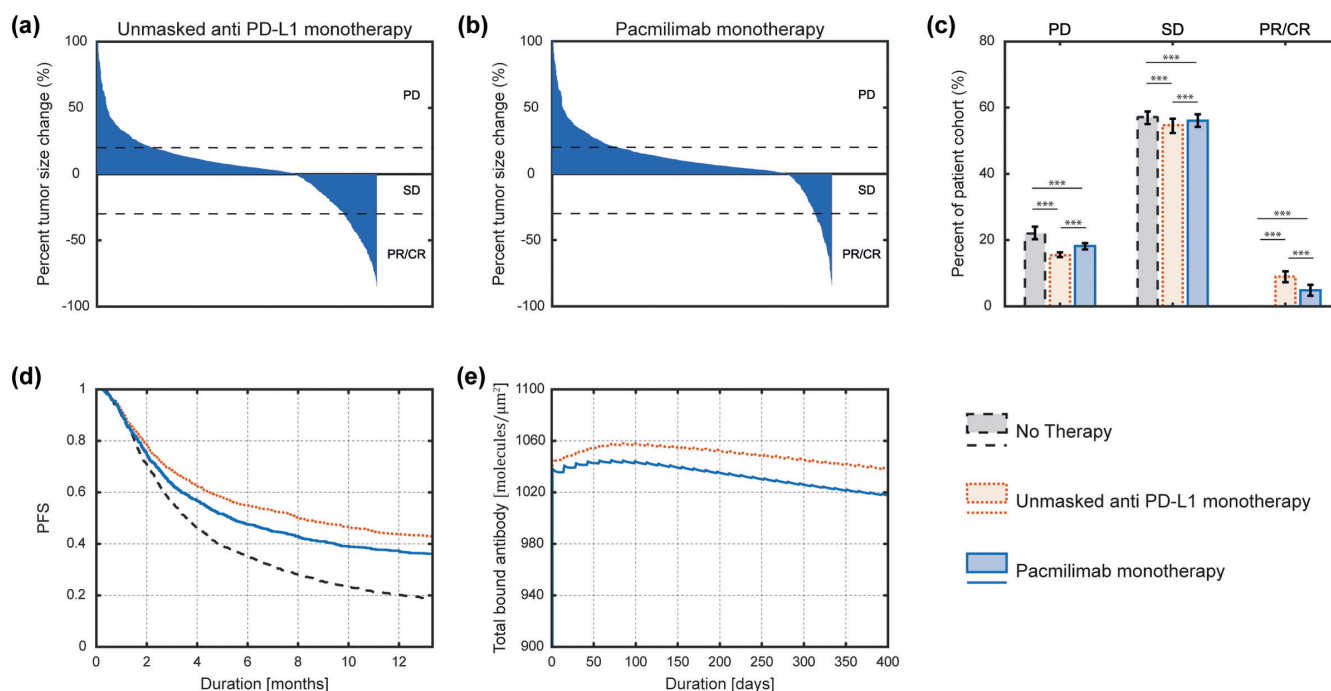


**FIGURE 3** Response, in terms of percent tumor change for the unmasked (a) and PbTx (b) anti-PD-L1 monotherapy. The same simulated patient cohort ( $N=1000$ ) is treated with each procedure following the same dosing schedule of 10 mg/kg q2w. The PbTx monotherapy appears to be slightly less effective than the unmasked therapy, in accordance to.<sup>18</sup> (c) Bar plot obtained from applying the RECIST<sup>17</sup> criteria to the data from panels (a) and (b) as well as the reference “untreated” case. The chart clearly shows that a masked therapy has an intermediate effect in terms of efficiency. (d) PFS from the three cases, Untreated, unmasked and masked monotherapy. This graph again supports the same conclusions obtained from panel c. (e) Total surface density of bound antibody or PbTx to PD-L1. This plot shows suggests that the similar efficacy of the PbTx treatment despite a lower density in bound antibodies. *P* values are (\*\*\*) $p < 0.001$ ; \*\* $p < 0.01$ , \* $p < 0.05$ ). CR/PR, complete response/partial response; PbTx, Probody therapeutics; PD, progressive disease; PFS, progression-free survival; SD, stable disease.

for unmasked therapy compared to the PbTx monotherapy (by 2%,  $p$  value  $<0.001$ ). Additionally, this result is in accordance with previous preclinical studies, where the response rate of mice treated with pacmilimab was similar to those treated with the unmasked equivalent.<sup>18</sup> Compared to the published phase I trial,<sup>6</sup> we report similar response rates to pacmilimab, model prediction of 6% versus 7% in the trial.<sup>6</sup> However, we would like to emphasize that the response to masked immunotherapy and unmasked immunotherapy are similar because they are within the CIs of each other.

We next probe the time evolution profiles of the progression-free survival (PFS) shown in Figure 3d. As expected, the untreated case shows the lower bound of the response. The PFS of the masked and unmasked monotherapies appear to be very close at each timepoint with the PFS for unmasked drug being higher. Because this property is distributed in time, we hypothesize that there is a dynamic effect causing this difference. From our simulations we can capture the density of total bound antibody to the cancer cells, as shown in Figure 3e. Here, both the profiles of unmasked and masked monotherapies show an initial steep rise in binding due to the high affinity of the antibodies to bivalent binding to receptors, that is, preferential bivalent bonding promoted by the avidity. However, after the initial peak, it seems that the pacmilimab curve is similar to the unmasked case. This result is despite the masking mechanism of the PbTx, which reduces the exposure of the antibody active sites and, ultimately, reduces the affinity of the antibody to the receptor. Thus, because the PD end points are related to the free surface density of PD-L1, similar coverage of this receptor on the cancer cell surface induces a similar immunosuppression leading to a similar response.

## Masking the antibody increases tumor specificity of the compound activity

We have discussed the effects of masking antibodies in terms of the antitumor efficacy, but we have yet to understand whether the simulated activity of PbTx is more localized to the tumor. The localization of drug activity has been one of the most researched topics in recent years.<sup>2</sup> PbTx are designed to promote preferential activation of the therapeutics in the tumor. The key component that governs this localization in activity is the cleavability of the mask due to proteases found and overexpressed in the TME. Here, we proceed to evaluate how the interplay between reversible unmasking and local mask cleavability affect the localization of drug activity.

Multiple states of the pacmilimab molecule are active, as shown in Figure 4a, namely any state that has at least

one open active site. Hence, the active states are any of the PbTx molecules that have been cleaved at least once or those which have at least one active site revealed by the unmasking process. We denote the concentration of these states as  $[A]$ . We compare the ratio of the concentrations of active antibodies between different compartments. For example, in Figures 4b and 4d, we compare the ratio between active antibody concentration in the tumor  $[A]_T$  compartment with the peripheral  $[A]_P$  and central  $[A]_C$  compartments, respectively. These profiles are obtained by averaging the ratios over the entire cohort of VPs. Independently of the therapy, whenever a new dose is injected, the ratios  $[A]_T/[A]_P$  and  $[A]_T/[A]_C$  drop, due to high concentration of drug following administration and delay of distribution to the tumor. This delay is due to the transport timescales required for the molecules to reach the TME from the central compartment where they are initially injected. However, there seem to be differences in these profiles, where the ratios  $[A]_T/[A]_P$  and not only  $[A]_T/[A]_C$  are more regular, that is, demonstrate much less stark peaks, but also seem overall larger in value for the PbTx compared to the unmasked antibody. To quantify these differences, we calculate the respective area under the curve profiles in Figures 4c and 4e. In both these panels, the masked monotherapy is always greater than the unmasked anti-PD-L1 monotherapy profile (around 10% at the end of treatment), suggesting that masking the antibody has increased the relative exposure of active (unmasked or partially unmasked) molecules in the tumor with respect to the rest of the body. Interestingly, Figures 4f and 4g show the absolute value of the concentrations (nanomolar) of the active molecules in the tumor and peripheral compartments. In both cases, the amount of the masked monotherapy is always more than an order of magnitude smaller than the unmasked case in the peripheral compartment. However, we would like to emphasize that although the absolute values between masked and unmasked therapy concentration differ, the ratios between these are closer because the reduction factor in active form concentration due to masking is similar between compartments (although it is higher outside the tumor). This result is intriguing as it means that a similar antitumor response to the drug was simulated even if at any timepoint the amount of active antibody is much lower in the peripheral compartment.

## Influence of key biomarkers and Probody therapeutic parameters on patient response

We have discussed the efficacy and localization of the PbTx monotherapy. We now proceed to discuss the key

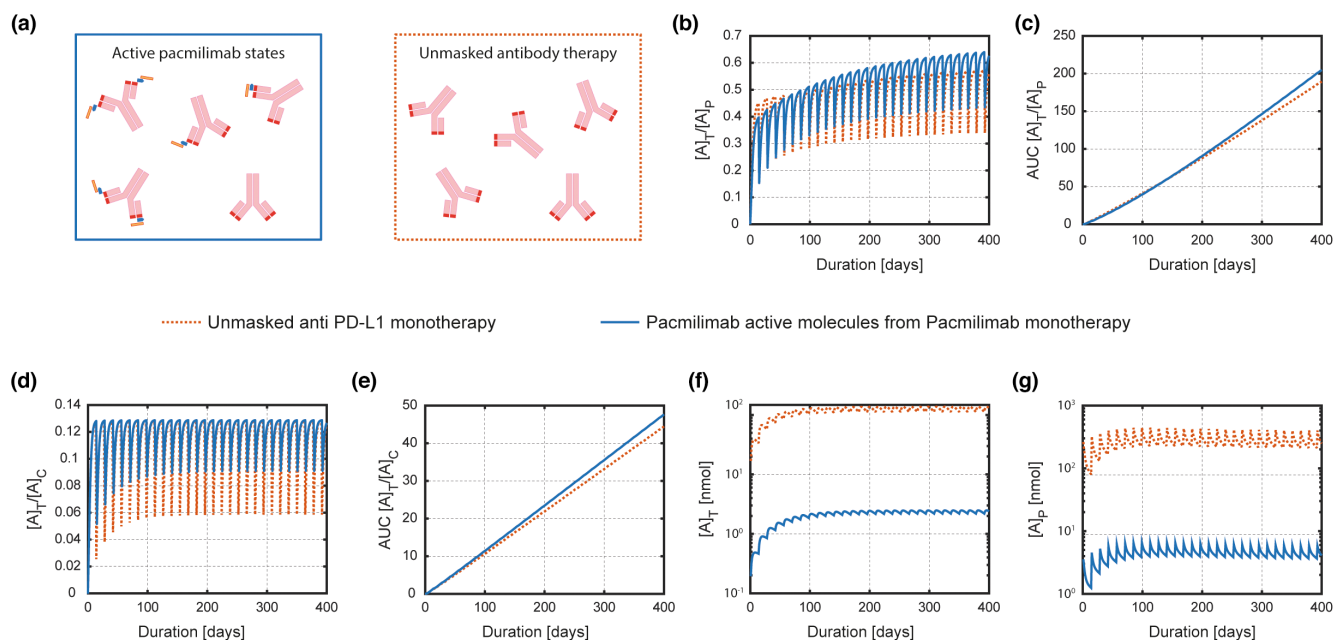


**FIGURE 4** (a) Cartoon showing the active states of the masked and unmasked antibodies. (b, d) These curves represent the ratios of the concentration of active antibody in the tumor compartment,  $[A]_T$ , with respect to the concentrations in the periphery,  $[A]_P$ , and blood,  $[A]_C$ . (c, e) are the respective AUC curves obtained from b and d. (c) The AUC for the PbTx monotherapy is higher than the unmasked therapy, suggesting a higher selectivity of the PbTx therapy. The same is true for (e), where in this case a higher AUC means a relatively lower concentration of active antibody is carried around the body. (f, g) These plots report the relative concentrations of active antibodies in the tumor (f) and periphery (g). In both cases, the PbTx curve is orders of magnitude below the unmasked case, which suggest that a similar efficacy is obtained even though the amount of active molecule circulating is much lower for PbTx therapies. AUC, area under the curve; PbTx, Probody therapeutics.

parameters or physical mechanisms governing the simulated patient response to pacmilimab.

As a first step, we ran a sensitivity analysis via partial rank correlation coefficient and report the results in Figure 5a.<sup>19</sup> Here, we study the correlation between the dependence of some key biomarkers, such as tumor size and immune cell densities, as a function of the patient dependent variables to determine which variable may govern response. The patient-dependent variables and their distributions can be found in Table S1. For each biomarker, we plot the five highest and five lowest correlation coefficients. From these, we are interested in measuring the key biomarkers included in pacmilimab dynamics, such as PD-L1 expression, PD-L2/PD-L1 ratio, as well as the dependence on the patient variable  $k_{cvg}$ . Throughout the analysis, we find that PD-L1 expression and the cleavage rate  $k_{cvg}$  are not sensitive parameters for response. PD-L2/PD-L1 was a sensitive parameter and is correlated to increase in tumor size.

In addition to the sensitivity analysis, we also assessed the difference in distinct biomarkers between simulated responders and nonresponders. In particular, we assessed the CD8 (or effector T cells [Teff]), CD4, Treg densities, Teff/Treg and M1/M2 ratios under pre-treatment and post-treatment conditions, in Figure 5b.

From these panels, we see that T cell densities are higher in responders compared to nonresponders. Additionally, the Teff/Treg ratio is higher in responders. Finally, it appears that the M1/M2 ratio is higher in nonresponders, a characteristic of the model explained by Wang et al.<sup>11</sup> Briefly, whereas M2 macrophages exhibit immunosuppressive activities, there is a correlation between M1-like macrophages and immunosuppressive species, which was also observed clinically.<sup>11,22</sup> However, as mentioned in Wang et al.<sup>11</sup> the role of tumor-associated macrophages in immunotherapies needs to be better understood.<sup>23</sup>

We next integrate the information gained from the sensitivity analysis and generate boxplots to evaluate the effect of key biomarkers of our simulated data on the objective response rate (ORR). In Figure 5c, for selected biomarkers we divide the patient cohort into two subgroups, that is, patients with the biomarker value above the median versus the rest. Hence, each subgroup will have exactly half of the total number of patients, although the subgroups for different biomarkers may not contain the same patients. Additionally, in this plot, the 95% CIs for ORR are shown which are obtained via bootstrapping. For comparison, we show as a dotted line the ORR obtained from the entire simulated patient cohort. Simulations suggest that



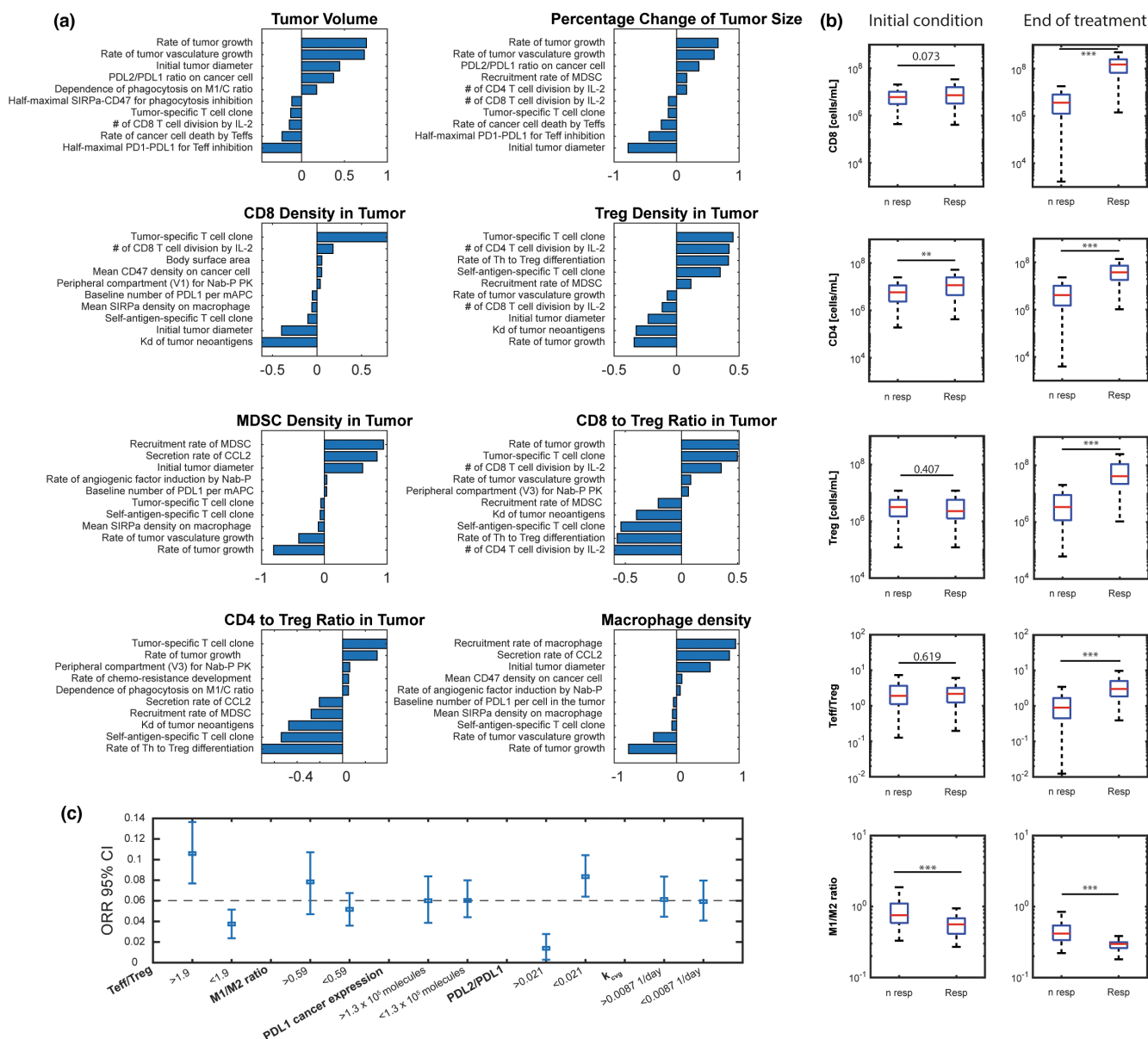


**FIGURE 5** (a) Sensitivity analysis describing the key patient-dependent parameters that affect important observables. (b) Summary of the biomarkers of responders and nonresponders before and after the PbTx monotherapy treatment. (c) Division into subgroups of the patient cohort to determine which biomarker or patient-dependent parameter affects the ORR. Each data point is built by bootstrapping from the relative half of the cohort ( $N=500$ ) and the error bars represent the 95% CI. CI, confidence interval; ORR, objective response rate; PK, pharmacokinetic; PbTx, Probody therapeutics.

a higher Teff/Treg ratio is associated with increased ORR. This result is expected as Teff are the main cell types for cytolytic activity against tumor cells, whereas the Tregs function as inhibitors of the immune response. Similarly, a higher M1/M2 ratio seems to be associated with higher ORR. On the other hand, PD-L1 expression on cancer cells does not strongly affect the ORR. This result corroborates the absence of PD-L1 expression as a significant variable in the overall sensitivity analysis. This is in line with studies in literature that report that PD-L1 expression on

cancer cells is rather controversial as a biomarker in determining antitumoral response.<sup>24</sup> However, a high PD-L2/PD-L1 ratio seems to be associated with a reduction in ORR. This result is due to the PD-L2 acting as an immune checkpoint for PD-1 while not binding to the PbTx molecule. Thus, more PD-L2 means more unchecked ligands that inhibit the immune response. Finally, the panel suggests that there is no correlation between higher cleavage rate and higher ORR, but this could be due to the small interpatient variability.

## Exploratory study with our QSP model suggests Proboddy therapeutic molecule characteristics and alternative dosing schedule

We have assumed that the PbTx parameters relate to those published in the literature and that the dosing schedule is fixed to the 10 mg/kg q2w. We next explore the possibility of changing the design features of the PbTx molecule to potentially improve antitumor response. To this end, we vary the two parameters  $K_M$ , the equilibrium constant describing the unmasking, and average  $k_{cvg}$  while keeping the rest of the PbTx parameters, such as the transport and clearance rates, the same as previously

calibrated parameters for atezolizumab.<sup>11</sup> We vary only these two parameters because they are the PbTx-specific parameters. The results are summarized in the table shown in Figure 6a–d, where we plot the change in ORR as a function of the ratio  $K_M/K_{ref}$  and  $k_{cvg}/k_{ref}$ , where  $K_{ref}$  and  $k_{ref}$  are the reference values of the PbTx parameters used in the previous simulations and reported in Tables S1 and S2. Simulations suggest that increasing  $K_M$  and  $k_{cvg}$  increases the ORR. This is an expected result as increasing these two parameters makes the PbTx more likely to be unmasked in the tumor.

During the phase I trial mentioned in ref. 6, the maximum dose tested in patients was 30 mg/kg scheduled q2w and the previous dose, with the same frequency, was

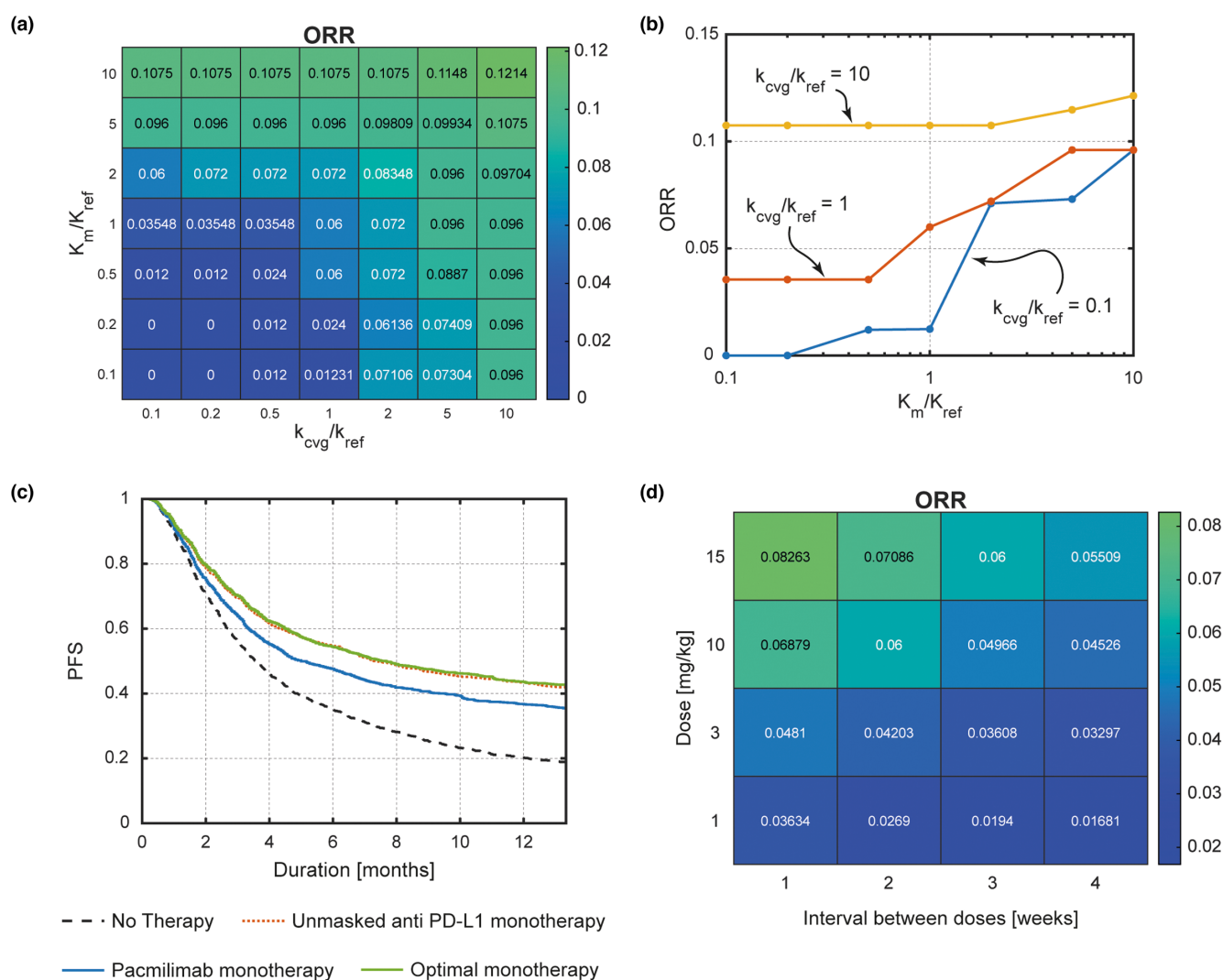


**FIGURE 6** (a) Table showing the variation of the ORR as a function of  $K_M$  versus  $k_{cvg}$ .  $K_{ref}$  and  $k_{ref}$  refer to the unmasking and average cleavage rates reported by Stroh et al.<sup>8</sup> The table shows that the ORR increases as  $K_M$  and  $k_{cvg}$  increases. (b) Selected ORR dependencies on  $K_M$  parametrized by a fixed  $k_{cvg}$ . (c) This is the same PFS reported in Figure 2c with the addition of the PFS for a reported therapy of  $K_M/K_{ref} = 10$  and the average  $k_{cvg}/k_{ref} = 10$ . (d) Effect on the ORR of the dosing schedule for masked monotherapy. The ORR increases as the dose increases or the interval between doses decreases. There were 1000 for each data point or curve. ORR, objective response rate; PFS, progression-free survival.

10 mg/kg. Here, we now aim to use the predictive power of the model to explore whether changing the dose level or dose frequency varies the response to the therapy. The summary of our simulations is shown in [Figure 6d](#), where we explored doses of 1, 3, 10, and 15 mg/kg with frequencies ranging q1w, q2w, q3w, and q4w. Each (pair of dose and dosing interval) contains at least 1000 simulated VPs. Two clear trends emerged. For a fixed interval, a higher dose seems to give higher response. On the other hand, for a fixed dose, longer intervals tend to give a lower response. Compared to the reference case of 10 mg/kg every q2w, increasing the dose to 15 mg/kg and reducing the interval to q1w increases the response by only about 30%, that is, from an ORR of 0.06 compared to the maximum ORR 0.08. However, we emphasize that these results do not account for increased probability of toxicities, not modeled in our framework, that may occur from higher exposure to the molecule.

## DISCUSSION AND CONCLUSIONS

In this paper, we have modified a QSP-IO model to study the effects of pacmilimab, a conditionally activated PD-L1 blocking antibody, applied to TNBC. We have used the model to compare the efficacy and tumor localization between a masked and unmasked antibody. Clinical trials have shown pacmilimab 10 mg/kg comparing favorably to historical data from PD-L1 or PD-1 inhibitors in patient populations unselected for PD-L1 expression<sup>25</sup> Niang et al.<sup>6</sup> have reported the ORR as 7%, similar to atezolizumab in patients with metastatic tumors, even though patients in that study did not exhibit high PD-L1 expression.<sup>26</sup> Our simulations corroborate that the efficacy induced by pacmilimab therapy is similar to the unmasked version. However, although our patient response percentages are close to the ones reported in clinical trials,<sup>6</sup> our waterfall plots in [Figure 2b](#) do not exactly match the ones reported by Niang et al.<sup>6</sup> This mismatch could be due to a number of reasons. For example, our model considers a single lesion, whereas, in general, the RECIST criteria can be applied to metastatic tumors. Additionally, the number of patients in our simulations are different from those reported by Niang et al.<sup>6</sup> The model also suggests that masking improves tumor localization of the drug. The preferential localization and similar response rate are in agreement with experiments performed on mice.<sup>18</sup> Additionally, our simulations suggest that the PbTx monotherapy provides similar therapeutic benefit even though the local tumor concentration of active molecules is lower compared to the unmasked molecule. We also have shown how the key biomarkers, such as immune cell

densities, change between responders and nonresponders to this therapy. Simulations suggest that a higher ratio  $T_{eff}/T_{reg}$  ratio increases the ORR. This result is expected as  $T_{eff}$ s have antitumoral activity whereas the  $T_{regs}$  function as inhibitors of the immune response. Similarly, a higher M1/M2 ratio seems to be associated with higher ORR. On the other hand, PD-L1 expression on cancer cells does not strongly affect the ORR. This result corroborates the absence of PD-L1 expression as a significant variable in the overall sensitivity analysis. This is in line with studies in literature that report that PD-L1 expression on cancer cells is rather controversial as a biomarker in determining antitumoral response.<sup>22</sup> However, a high PD-L2/PD-L1 ratio seems to strongly reduce the ORR. This result is due to the PD-L2 acting as an immune-checkpoint for PD-1 while not binding to the PbTx molecule. Thus, more PD-L2 means more unchecked ligands that inhibit the immune response. Additionally, our framework allowed us to run an exploratory study on the design parameters of the PbTx kinetics and of the dosing schedule to determine the combination that maximizes the ORR.

There are some limitations to this study which we aim to overcome in future work. For example, cancer associated fibroblasts (CAFs) are not accounted for in our model. CAFs are fibroblasts which via cytokine signaling, such as  $IFN-\gamma$ ,<sup>27</sup> polarize and strengthen the cancer against antitumoral stimuli. This pro-tumorigenic activity is known to occur via extracellular matrix remodeling, which provides a physical barrier to the infiltration of T cells and reduced cancer cell exposure to immunotherapies,<sup>28,29</sup> and by the release of growth factors, such as HGF<sup>30</sup> or other cytokines which stimulate tumor progression. In fact, because most of the activation due to protease activity occurs in the TME, the barrier to the penetration of therapeutic agents due to CAFs could influence the PbTx therapy's efficacy. Additionally, although we have included the out-of-synapse dynamics, we have not included any specific interactions between the antibody and PD-L1 that are known to lead to downstream effects.<sup>12</sup> The QSP modeling platform described here can be readily extended to include other cancer types or other PbTx checkpoint inhibitors by adapting the appropriate parameters, such as the ones describing the cancer module (see [Appendix S1](#)), the kinetics of the PbTx, such as the cleavage rate, which may be cancer dependent,<sup>27</sup> or other parameters that govern binding, unbinding, and tumor penetration of the molecule. Another limitation of the model is due to the lack of explicit modeling of the toxicities associated with the therapy. However, evidence from literature and the relative exposures to active molecules from our results suggest that the PbTx molecule's conditionality obtained

from masking will reduce the toxicity. We aim to extend the model in future work to include toxicity effects to further evaluate the potential of conditionally activated therapies. Additionally, the framework described in this work is valid for single lesion tumors, whereas, in general, RECIST scores also depend on metastases. Recent perspectives have also suggested the importance of including multiple lesions because they are critical in understanding RECIST scores.<sup>31</sup> Arulraj et al.<sup>32</sup> have used omics data to extend a single lesion QSP model to include multiple metastases. This framework could be extended to this setting to evaluate the effects of a PbTx therapy for metastatic tumors, considering lesion-to-lesion parameter differences, such as the cleavage rate.

Overall, in this work, we have provided a platform to describe the activation of the cancer immunity cycle in response to a PD-L1 blocking PbTx and we have demonstrated its predictive potential. Moreover, the framework allows for exploration of design criteria for the PbTx to optimize its activation in the tumor microenvironment.

## AUTHOR CONTRIBUTIONS

All authors wrote and/or reviewed and edited the manuscript. A.I., H.B., and A.S.P. designed the research. A.I. performed the research. A.I. analyzed the data. A.I. and H.W. contributed new analytical tools.

## ACKNOWLEDGMENTS

PROBODY is a US registered trademark of CytomX Therapeutics, Inc. We thank Drs. Cathrine Leonowens, and Dylan Daniel for their constructive comments.

## FUNDING INFORMATION

This study was funded by CytomX Therapeutics, Inc., South San Francisco, CA. It was also supported in part by NIH grants R01CA138264 and U01CA212007 (A.S.P.).


## CONFLICT OF INTEREST STATEMENT

H.B. and V.V. are CytomX Therapeutics employees. The other authors declare no competing interests for this work.

## ORCID

Hanwen Wang  <https://orcid.org/0000-0001-5480-431X>

Yu Zhang  <https://orcid.org/0000-0003-3643-6589>

Aleksander S. Popel  <https://orcid.org/0000-0002-6706-9235>

## REFERENCES

- Desnoyers LR, Vasiljeva O, Richardson JH, et al. Tumor-specific activation of an EGFR-targeting probody enhances therapeutic index. *Sci Transl Med*. 2013;5(207):207ra144.
- Kavanaugh WM. Antibody prodrugs for cancer. *Expert Opin Biol Ther*. 2020;20(2):163-171.
- Wong KR, Menendez E, Craik CS, Kavanaugh WM, Vasiljeva O. In vivo imaging of protease activity by Probody therapeutic activation. *Biochimie*. 2016;122:62-67.
- Naing A, Thistlethwaite FC, Spira AI, et al. CX-072, a PD-L1 Probody therapeutic, as monotherapy in patients with advanced solid tumors: preliminary results of PROCLAIM-CX-072. *J Clin Oncol*. 2019;37(15\_Suppl):2513.
- Autio KA, Arkenau HT, O'Neil BH, et al. Preliminary results of the first-in-human, dose-finding PROCLAIM-CX-072 trial of the PD-L1 Probody therapeutic CX-072 as monotherapy in patients (pts) with advanced solid tumors. *J Clin Oncol*. 2018;36(15 suppl):3071.
- Naing A, Thistlethwaite F, De Vries EG, et al. CX-072 (pac-milimab), a Probody® PD-L1 inhibitor, in advanced or recurrent solid tumors (PROCLAIM-CX-072): an open-label dose-finding and first-in-human study. *J Immunother Cancer*. 2021;9(7):e002447.
- Stroh M, Sagert J, Burke JM, et al. Quantitative systems pharmacology model of a masked, tumor-activated antibody. *CPT Pharmacometrics Syst Pharmacol*. 2019;8(9):676-684.
- Stroh M, Green M, Millard BL, et al. Model-informed drug development of the masked anti-PD-L1 antibody CX-072. *Clin Pharmacol Therapeut*. 2021;109(2):383-393.
- Bai JP, Earp JC, Pillai VC. Translational quantitative systems pharmacology in drug development: from current landscape to good practices. *AAPS J*. 2019;21(4):1-3.
- Bradshaw EL, Spilker ME, Zang R, et al. Applications of quantitative systems pharmacology in model-informed drug discovery: perspective on impact and opportunities. *CPT Pharmacometrics Syst Pharmacol*. 2019;8(11):777-791.
- Wang H, Zhao C, Santa-Maria CA, Emens LA, Popel AS. Dynamics of tumor-associated macrophages in a quantitative systems pharmacology model of immunotherapy in triple-negative breast cancer. *iScience*. 2022;25(8):104702.
- Escors D, Gato-Cañas M, Zuazo M, et al. The intracellular signalosome of PD-L1 in cancer cells. *Signal Transduct Target Ther*. 2018;3(1):1-9.
- Bazzazi H, Shahraz A. A mechanistic systems pharmacology modeling platform to investigate the effect of PD-L1 expression heterogeneity and dynamics on the efficacy of PD-1 and PD-L1 blocking antibodies in cancer. *J Theor Biol*. 2021;522:110697.
- Cheng X, Veverka V, Radhakrishnan A, et al. Structure and interactions of the human programmed cell death 1 receptor. *J Biol Chem*. 2013;288(17):11771-11785.
- Vasiljeva O, Menendez E, Nguyen M, Craik CS, Michael Kavanaugh W. Monitoring protease activity in biological tissues using antibody prodrugs as sensing probes. *Sci Rep*. 2020;10(1):5894.
- Bhatt AS, Takeuchi T, Ylstra B, et al. Quantitation of membrane type serine protease 1 (MT-SP1) in transformed and normal cells. *Biol Chem*. 2003;384:257-266.
- Gilbar PJ, Davis MR. Dosing of PD-1 and PD-L1 inhibitors: cost saving initiatives for significantly decreasing associated expenditure. *J Oncol Pharm Pract*. 2021;27(1):199-204.
- Chan P, Marchand M, Yoshida K, et al. Prediction of overall survival in patients across solid tumors following atezolizumab treatments: a tumor growth inhibition-overall survival modeling framework. *CPT: Pharmacometrics & Systems Pharmacology*. 2021;10(10):1171-1182.



19. Eisenhauer EA, Therasse P, Bogaerts J, et al. New response evaluation criteria in solid tumours: revised RECIST guideline (version 1.1). *Eur J Cancer*. 2009;45(2):228-247.
20. Assi HH, Wong C, Tipton KA, et al. Conditional PD-1/PD-L1 Probody therapeutics induce comparable antitumor immunity but reduced systemic toxicity compared with traditional anti-PD-1/PD-L1 agents. *Cancer Immunol Res*. 2021;9(12):1451-1464.
21. Marino S, Hogue IB, Ray CJ, Kirschner DE. A methodology for performing global uncertainty and sensitivity analysis in systems biology. *J Theor Biol*. 2008;254(1):178-196.
22. Oshi M, Tokumaru Y, Asaoka M, et al. M1 macrophage and M1/M2 ratio defined by transcriptomic signatures resemble only part of their conventional clinical characteristics in breast cancer. *Sci Rep*. 2020;10(1):1-2.
23. Xiang X, Wang J, Lu D, Xu X. Targeting tumor-associated macrophages to synergize tumor immunotherapy. *Signal Transduct Target Ther*. 2021;6(1):1-2.
24. Doroshov DB, Bhalla S, Beasley MB, et al. PD-L1 as a biomarker of response to immune-checkpoint inhibitors. *Nat Rev Clin Oncol*. 2021;18(6):345-362.
25. Zhao B, Zhao H, Zhao J. Efficacy of PD-1/PD-L1 blockade monotherapy in clinical trials. *Therapeut Adv Med Oncol*. 2020;12:1758835920937612.
26. Emens LA, Cruz C, Eder JP, et al. Long-term clinical outcomes and biomarker analyses of atezolizumab therapy for patients with metastatic triple-negative breast cancer: a phase 1 study. *JAMA Oncol*. 2019;5(1):74-82.
27. Subramaniam KS, Tham ST, Mohamed Z, Woo YL, Mat Adenan NA, Chung I. Cancer-associated fibroblasts promote proliferation of endometrial cancer cells. *PLoS One*. 2013;8(7):e68923.
28. Salmon H, Franciszkiwicz K, Damotte D, et al. Matrix architecture defines the preferential localization and migration of T cells into the stroma of human lung tumors. *J Clin Invest*. 2012;122(3):899-910.
29. Kuczek DE, Larsen AM, Thorseth ML, et al. Collagen density regulates the activity of tumor-infiltrating T cells. *J Immunother Cancer*. 2019;7(1):1-5.
30. Jia CC, Wang TT, Liu W, et al. Cancer-associated fibroblasts from hepatocellular carcinoma promote malignant cell proliferation by HGF secretion. *PLoS One*. 2013;8(5):e63243.
31. Kumar R, Qi T, Cao Y, Topp B. Incorporating lesion-to-lesion heterogeneity into early oncology decision making. *Front Immunol*. 2023;14:1173546.
32. Arulraj T, Wang H, Emens LA, Santa-Maria CA, Popel AS. A transcriptome-informed QSP model of metastatic triple-negative breast cancer identifies predictive biomarkers for PD-1 inhibition. *Sci Adv*. 2023;9(26):eadg0289.

## SUPPORTING INFORMATION

Additional supporting information can be found online in the Supporting Information section at the end of this article.

**How to cite this article:** Ippolito A, Wang H, Zhang Yu, Vakil V, Bazzazi H, Popel AS. Eliciting the antitumor immune response with a conditionally activated PD-L1 targeting antibody analyzed with a quantitative systems pharmacology model. *CPT Pharmacometrics Syst Pharmacol*. 2024;13:93-105. doi:[10.1002/psp4.13060](https://doi.org/10.1002/psp4.13060)